Altered Mitochondrial Dynamics, Biogenesis, and Functions in the Paclitaxel-Resistant Lung Adenocarcinoma Cell Line A549/Taxol

Authors' Contribution:
Study Design A
Data Collection B
Statistical Analysis C
Data Interpretation D
Manuscript Preparation E
Literature Search F
Funds Collection G

F **Xiang Zhou***
B **Rui Li***
C **Ruohua Chen**
A **Jianjun Liu**

Department of Nuclear Medicine, Renji Hospital, School of Medicine, Shanghai Jiao Tong University, Shanghai, P.R. China

Corresponding Author:
Source of support:

* Xiang Zhou and contributed to this work equally
Jianjun Liu, e-mail: jianjun_liu2018@163.com
This work is supported by grants from the National Natural Science Foundation of China (No. 81571710, 30830038, 30970842, 81071180 and 81601520)

Background: Chemoresistance is a primary hindrance for current cancer treatments. The influence of abnormal mitochondria in chemotherapy resistance is not well known. To explore the correlation between mitochondria and acquired chemoresistance, this work studied alterations in mitochondrial dynamics, biogenesis, and functions for paclitaxel-resistant cancer cell line A549/Taxol and its parental line A549.

Material/Methods: Mitochondrial morphology was observed by transmission electron microscopy and confocal microscopy. We measured the mitochondrial mass and mitochondrial membrane potential using fluorescent dyes. The glucose metabolic profile and ATP (adenosine triphosphate) content were determined by bioluminescent cell assays. Seahorse bio-energy analyzer XF24 was used to detect the mitochondrial respiratory function. The expressions of mitochondrial dynamics and biogenesis related genes were quantified using real-time polymerase chain reaction.

Results: We observed fusion morphology of the mitochondrial network in A549/Taxol cells, with upregulation of fusion genes (Mfn1 and Mfn2) and downregulation of fission gene Fis1. In A549/Taxol cells, mitochondrial mass showed a significant decrease, while the mitochondrial biogenesis pathway was strongly activated. Despite the decreased mitochondrial membrane potential, the capability for mitochondrial respiration was not impaired in A549/Taxol cells.

Conclusions: Our study revealed a series changes of mitochondrial characteristics in paclitaxel-resistant cells. Mfn1 and Mfn2 and PGC-1α increased, while Fis1 expression and mitochondrial oxidative phosphorylation decreased in A549/Taxol cell lines. These changes to mitochondrial fusion, fission, and biological function contributed to the occurrence of paclitaxel resistance in tumor cells which induced paclitaxel resistance.

MeSH Keywords: Drug Resistance • Energy Metabolism • Lung Neoplasms • Mitochondria • Paclitaxel

Abbreviations: **2-DG** – 2-deoxy-D-glucose; $\Delta\psi_m$ – mitochondrial membrane potential; **DRP1** – dynamin-related protein 1; **ECAR** – extracellular acidification rate; **ERR**α – estrogen-related receptor α; **FCCP** – carbonyl cyanide p-[trifluoromethoxy]-phenyl-hydrazone; **Fis1** – mitochondrial fission 1; **JC-1** – 5,5',6,6'-tetrachloro-1,1',3,3'-tetraethylbenzimidazolylcarbocyanine iodide; **Mfn** – mitofusin; **NRF** – nuclear respiratory factor; **NSCLC** – non-small cell lung cancer; **OCR** – oxygen consuming rate; **OPA1** – optic atrophy 1; **OXPHOS** – oxidative phosphorylation; **PGC** – peroxisome proliferator-activated receptor-γ coactivator; **PPAR**α – peroxisome proliferator-activated receptor α; **RCR** – respiratory control ratio

Full-text PDF: https://www.medscimonit.com/abstract/index/idArt/918216

📄 3386   📊 1   📈 3   📚 43

Background

Despite a reported decline in recent years, lung cancer is still the second most common cancer type [1]. Non-small cell lung cancer (NSCLC) is the most common malignant form of lung cancer, accounting for approximately 75% to 80% of all lung cancer cases throughout the world [2,3]. Paclitaxel is widely used as one of first-line chemotherapy reagents for NSCLC, breast cancer, and ovarian cancer [4–6]. Despite good initial response, NSCLC patients who receive paclitaxel treatment often develop acquired chemoresistance, which greatly decreases clinical efficacy. A range of molecular mechanisms has been identified to explain the paclitaxel resistance, including overexpression of multidrug resistance proteins, β-tubulin isoform changes and apoptosis pathway regulation [7,8]. However, none of these mechanisms can completely account for paclitaxel resistance.

Abnormal changes to mitochondria have been proven to be involved in the pathogenesis of cancer and other diseases [9]. Mitochondrial malfunctions have been shown to be associated with tumorigenesis and tumor metastasis, and probably play a role in cancer therapy resistance [10–12]. It has been proposed that mitochondria could use microtubule networks as railways to translocate within cells, and studies have confirmed that the intracellular distribution and biogenesis of mitochondria could be affected by microtubule drugs [13]. Thus, we assumed mitochondrial profiles would change correspondingly in paclitaxel- resistant cancer cells.

A549/Taxol cells are paclitaxel-resistant A549 cells. In our previous study, we observed that DCA (dichloroacetate) can target A549/Taxol cells and enhance the sensitivity to paclitaxel [10]. Considering DCA can target cells with mitochondrial injury, we wanted to make clear whether mitochondrial of A549/Taxol cells was damaged. Mitochondrial injury may be associated with changes in mitochondrial biosynthesis, mitochondrial fusion, mitotic function, mitochondrial membrane potential, ATP (adenosine triphosphate) production, etc. [10,14]. These changes in mitochondria are closely related to anti-tumor drug resistance. In this study, we used the lung adenocarcinoma cell line A549 and its paclitaxel-resistant subline A549/Taxol to analyze mitochondrial alterations, and suggested that there might be a mitochondria-related mechanism involved in the acquisition of paclitaxel resistance.

Material and Methods

Cell culture

A549 cell line was purchased from the Cell Bank of the Chinese Academy of Sciences (Shanghai, China) and A549/Taxol cell line from the Basic Research Laboratory of Shanghai Chest Hospital [15]. A549 and A549/Taxol cells were grown at 37°C in a humidified atmosphere with 5% CO_2 in high glucose Dulbecco's Modified Eagle Medium (DMEM; GIBCO, Life Technologies) supplemented with 5% fetal bovine serum (FBS; GIBCO, Life Technologies).

Cell viability and proliferation assays

Cells were seeded into 96-well plates at 3.0×10^3 cells/well. After culturing at 37°C for 24 hours, cells were exposed to paclitaxel (Taxol, Bristol-Myers Squibb) at doses of 1, 2, 5, 10, 20, 40, 80, 160, 320, 640, 1280, and 2000 µg/L for 48 hours. The control group and the blank group were set at the same time. Cell viability was detected by Cell Counting Kit-8 (CCK-8; TaKaRa Biotechnology). The optical density was measured at 450 nm on a multimode microplate reader Infinite 200 PRO (TECAN). The IC50 of paclitaxel was calculated. Cells were seeded into 96-well plates at 2.0×10^3 cells/well and incubated. Five samples were used for cell counting every 24 hours, and growth curves were plotted after a week. Doubling time was calculated.

Transmission electron microscopy (TEM) and image analysis

Cells were pre-fixed with 2.5% glutaraldehyde in 0.2 mol/L cacodylate buffer for 2 hours at 4°C and then released from the plastic culture dish by gentle scraping. After washing with 0.1 mol/L cacodylate buffer 3 times, being post-fixed in 1% osmium tetroxide for 2 hour and dehydrated in ethanol, cells were embedded in epoxy resin. Ultrathin sections were placed on copper grids, stained with uranyl acetate and lead citrate, and then examined in a CM-120 BioTwin transmission electron microscope (Philips). Then 30 TEM images of A549 and A549/Taxol were captured, respectively. We evaluated and calculated the average mitochondrial size.

Confocal laser scanning microscopic analysis of mitochondrial morphology and mitochondrial membrane potential ($\Delta\psi_m$)

Cells growing in 35 mm coverglass-bottom confocal dishes were incubated with 100 nmol/L of Mito Tracker Red CMXRos (Molecular Probes, Life technologies) in the dark for 20 minutes at 37°C. This dye can selectively accumulate in active mitochondria. Mitochondrial morphology was observed using an LSM-510 laser scanning confocal microscope (Zeiss). To determine the $\Delta\psi_m$, cells were stained with 100 µg/mol of JC-1 (Sigma) in the dark for 20 minutes at 37°C. In cells with high $\Delta\psi_m$, JC-1 spontaneously forms J-aggregates with orange fluorescence. JC-1 remains in a monomeric form with green fluorescence when $\Delta\psi_m$ remains low.

Table 1. Primers used for real-time quantitative polymerase chain reaction.

Gene	Sense primer	Antisense primer
DRP1	5'-AAATCGTCGTAGTGGGAACGCAGA-3'	5'-TGGACCAGTTGCAGAATGAGAGGT-3'
Fis1	5'-TGAAGAAAGATGGACTCGTGGGCA-3'	5'-ACTTGGACACAGCAAGTCCGATGA-3'
Mfn1	5'-CAAGGTGAATGAGCGGCTTTCCAA-3'	5'-ATGCAGGCATCTTTCCATGTGCTG-3'
Mfn2	5'-TGTCTGGGACCTTTGCTCATCTGT-3'	5'-TTCCTGAGCAGCTTTGCTTTGCTC-3'
OPA1	5'-GCATGCTAAAGGCACACCAAGTGA-3'	5'-TTCCCGCAGGCGAGGATAGTTATT-3'
PGC-1α	5'-AACAGCAGCAGAGACAAATGCACC-3'	5'-TGCAGTTCCAGAGAGTTCCACACT-3'
PGC-1β	5'-CTCCATTCTGAGGGAACTTCTG-3'	5'-GTGTGAGGGAGGCATAAACA-3'
NRF1	5'-GAAACTTCGAGCCACGTTAGA-3'	5'-GTTAGGTTTGGAGGGTGAGATAC-3'
NRF2	5'-GCCCAGTCTTCATTGCTACT-3'	5'-GTCCTGTTGCATACCGTCTAA-3'
ERRα	5'-GAATGCACTGGTGTCTCATCT-3'	5'-GACCACAATCTCTCGGTCAAA-3'
PPARα	5'-CAAGGCCTCAGGCTATCATTAC-3'	5'-GTCGCACTTGTCATACACCA-3'
β-actin	5'-CAGGGCGTGATGGTGGGCA-3'	5'-CAAACATCATCTGGGTCATTCTC-3'

Flow cytometry analysis of mitochondrial mass and Δψm

The mitochondrial-selective probe Mito Tracker Green (MTG, Beyotime) was used to detect the mitochondrial mass. This dye could localize to mitochondria regardless of Δψm. Cells were incubated with 100 nmol/L of MTG dye in the dark for 20 minutes at 37°C, and immediately analyzed with a BD FACSAria flow cytometer (BD Biosciences). Cells were also incubated with 10 μg/mL of JC-1 in the dark for 20 minutes at 37°C, and quantified Δψm with flow cytometry analysis. The JC-1 ratio was calculated as the ratio of red fluorescence to green fluorescence.

Determination of cellular ATP production

Cells were seeded in 24-well plates at 3.0×10⁴ cells per well. After incubation for 48 hours, the cellular ATP level was determined with an ATP bioluminescent somatic cell assay kit (SIGMA). All procedures were carried out in accordance with the manufacturer's instructions. The amount of light emitted was measured immediately with Infinite 200 PRO, and the amount of ATP in each sample was calculated and normalized by cell numbers.

Determination of cellular glucose consumption and lactate production

Glucose consumption in 24 hours was measured with a glucose determination reagent (Shanghai Rongsheng Biotech Co., Ltd.), and lactate production in 24 hours was measured with a lactate reagent (CMA Microdialysis). All procedures were carried out in accordance with the manufacturer's instructions.

Determination of mitochondrial respiratory function

XF24 Extracellular Flux Analyzer (Seahorse Biosciences) was used to detect mitochondrial respiration. After initial optimization of experimental conditions, cells were seeded at 2.0×10⁴ cells per well and cultured for 24 hours before measurement. The respiratory function of live mitochondria was determined by assessing the oxygen consumption rate (OCR) and extracellular acidification rate (ECAR) [16]. Cells were sequentially exposed to 3 chemicals: oligomycin (1 μmol/L), carbonyl cyanide p-[trifluoromethoxy]-phenyl-hydrazone (FCCP) (1 μmol/L), and rotenone/antimycin (1 μmol/L). It is important to note that oligomycin inhibits the F_1F_0-ATP synthase and therefore decreases mitochondrial respiration and increases glycolysis. FCCP is an uncoupler of electron transport and mitochondrial respiration and could be used to investigate the cellular respiratory reserve capacity (RCR). Rotenone and antimycin, as inhibitors of electron transport chain complex I and III, are mixed together to completely eliminate mitochondrial respiration.

Real-time quantitative polymerase chain reaction (PCR)

The total RNA of cells was extracted according to protocols for the E.Z.N.A Total RNA kit I (OMEGA Bio-Tek). Sample cDNAs were then processed using reverse transcription with 1 μg total RNA using PrimeScript® RT reagent Kit (TaKaRa Biotechnology). Real-time PCR was performed with a Roche LightCycler® 480 system (Roche Applied Science). The specific primers used were shown in Table 1. The expression of genes of interest was normalized against that of the housekeeping gene β-actin.

Statistics

All data were presented as mean±standard deviation (SD). Statistical analyses were performed using a Student's t-test. $P<0.05$ was taken as the level of significance. STATA Statistical Software Release 12.0 was used for all the statistical analysis.

Results

Validation of paclitaxel-resistant phenotype

A549/Taxol cells were paclitaxel-resistant A549 cells. To confirm the acquired paclitaxel-resistant phenotype, the IC50 of paclitaxel in A549 and A549/Taxol cells were determined first. After paclitaxel treatment, the IC50 value of A549 cells was 10.18±0.27 µg/L, while the IC50 value of A549/Taxol cells reached 248.68±1.67 µg/L ($P<0.01$). We next tested whether the development of paclitaxel resistance affected cell proliferation. The doubling time of A549 and A549/Taxol cells was 28.8±0.64 hours and 32.5±1.25 hours, respectively ($P<0.05$). A549/Taxol cells showed a slower proliferation rate compared with A549 cells, and this observation was similar with other acquired chemoresistance cells.

Measurement of mitochondrial morphology changes

As semi-autonomous organelles, mitochondria are capable of changing their size and shape through consistent fusion and division [16]. Paclitaxel, as a microtubule stabilizing agent, has been reported to alter the characteristics of mitochondrion and inhibit movement [17]. Thus, we questioned the possibility that mitochondrial morphology would change accordingly in paclitaxel-resistant cells. TEM revealed that mitochondria were enlarged in A549/Taxol cells in comparison to A549 cells (Figure 1A). No corresponding pathological alterations related to mitochondrial matrix swelling or cristae disintegration were observed. The average mitochondrial size in A549/Taxol cells was 0.12±0.05 µm^2, which was larger than A549 cells with an average of 0.08±0.04 µm^2 (Figure 1B). We further assessed the mitochondrial shape with confocal microscopy. Consistent with TEM results, mitochondria in A549/Taxol cells were obviously elongated and branched, while the morphology of mitochondria in A549 cells formed mostly punctuated structures (Figure 1C). To further verify this morphologic change, we detected gene expressions of mitochondrial dynamin-related proteins (Figure 1D). Mfn and OPA1 proteins are involved in mitochondrial fusion function, and Fst1 and DRP1 proteins regulates mitochondrial fission [14]. Our results show that the mRNA expressions of Mfn1 and Mfn2 were both upregulated in A549/Taxol cells, with an almost 2-fold increase compared to A549 cells. Meanwhile, A549/Taxol cells exhibited a lower expression level of Fis1 than A549 cells. However,

both DRP1 and OPA1 expressions did not exhibit any statistically significant differences. This data further confirmed the morphological changes observed under TEM and confocal microscopy, indicating that mitochondria in A549/Taxol cells adopted a more fused status than in A549 cells, which may partly explain the increased mitochondrial size.

Measurement of changes in mitochondrial biogenesis

To check mitochondrial biogenesis in the acquired chemoresistant phenotype, we quantified mitochondrial mass by flow cytometry. There was a significant decrease in mitochondrial mass in A549/Taxol cells when compared with A549 cells. Interestingly, mitochondrial mass remained constant in A549/Taxol cells after 12 hours incubation of Taxol (100 µg/L), while mitochondrial mass in A549 cells increased distinctly (Figure 2A). Strong evidence shows that the peroxisome proliferator-activated receptor gene family is the master regulator of mitochondrial biogenesis, which generally lead to mitochondrial mass and size changes [18,19]. Nuclear coactivators PGC-1α and PGC-1β regulate mitochondrial biogenesis and function by coordinating transcription factors and activating the mitochondrial retrograde signaling pathway [20]. The quantitative PCR results revealed that the transcription of PGC-1α was upregulated dramatically in A549/Taxol cells, while PGC-1β mRNA transcription did not show significant differences between the 2 cell lines (Figure 2B). The mRNA transcriptions of PGC-1α targets were also measured, NRF-1, NRF-2, ERRα, and PPARα were all upregulated in A549/Taxol cells (Figure 2C). It has been reported that NRF-1, NRF-2, and ERRα are involved in mitochondrial remodeling and restructuring [21–24]. These results indicated that A549/Taxol cells might compensate for the drastic reduction in mitochondrial mass by upregulating its mitochondrial biogenesis.

Measurement of $\Delta\psi_m$, energy metabolism, and mitochondrial respiratory function

Normal mitochondrial membrane potential maintains mitochondria for oxidative phosphorylation and ATP production, essential for maintaining mitochondrial function. When mitochondria are damaged, mitochondrial Oxidative phosphorylation (OXPHOS) activity and mitochondrial membrane potential decrease [25]. To determine the functional states of mitochondria, cells were first stained with JC-1 dye to detect $\Delta\psi_m$. Using confocal microscopy, we observed that the A549/Taxol cells exhibited a significant decrease in JC-1 staining compared to A549 cells (Figure 3A). We further quantified the $\Delta\psi_m$ by flow cytometry, revealing that red/green fluorescence intensity ratio reduced by approximately 50% in A549/Taxol cells when compared to A549 cells (Figure 3B). This result demonstrated that there were an increased proportion of depolarized mitochondria in A549/Taxol cells.
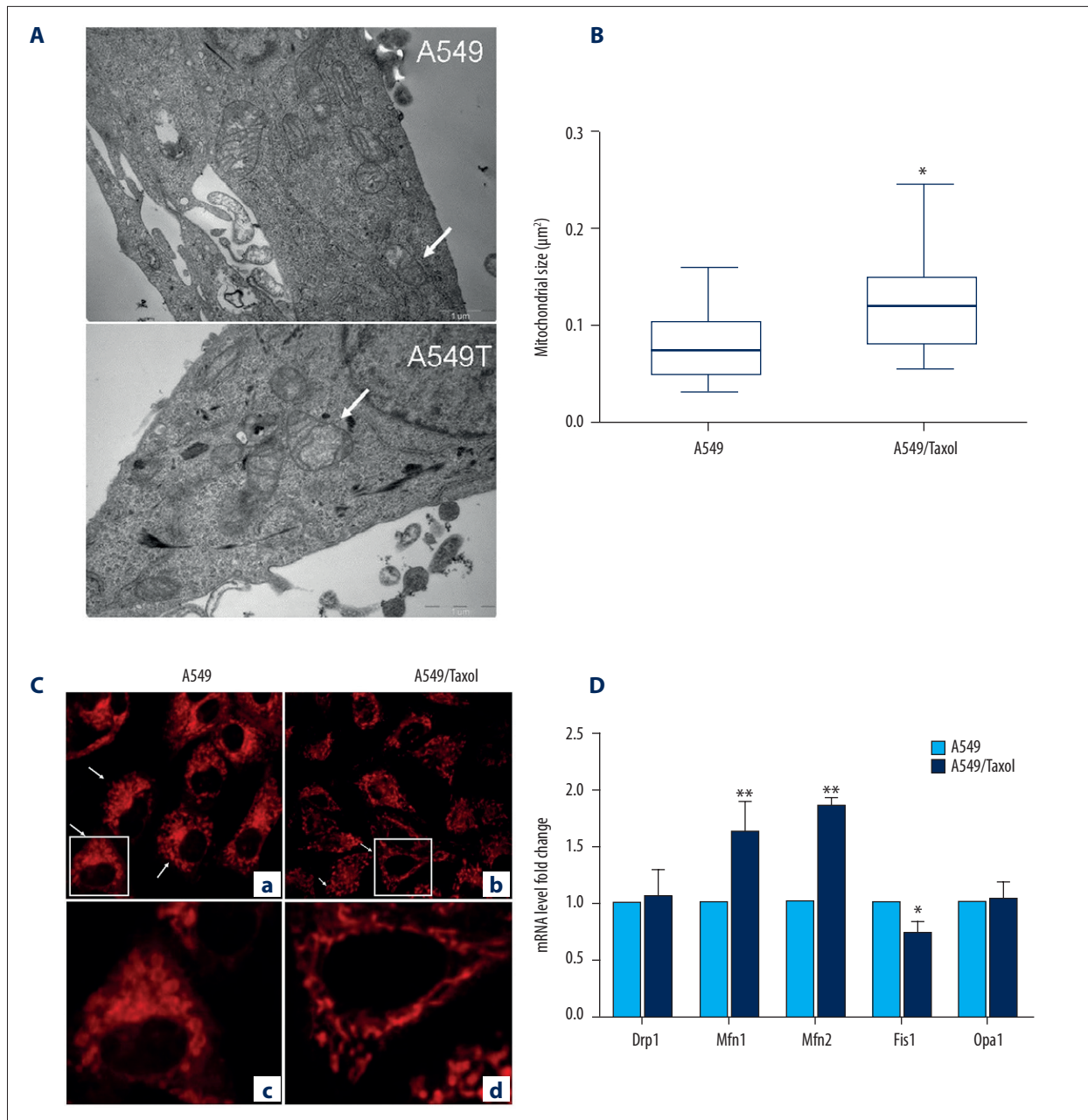
Figure 1. Mitochondrial morphologic and dynamic alterations in paclitaxel-resistant cells. (**A**) Ultrastructure of mitochondria was observed in A549 and A549/Taxol cells under transmission electron microscopy (TEM). Representative images of mitochondrial morphologic features (magnification, 20 000×). (**B**) Image analysis of average mitochondrial size in A549 and A549/Taxol cells; 30 TEM images of each cell line were calculated. (**C**) Representative confocal microscopy images of mitochondrial structure: (**a**) mitochondrial morphology in A549 cells; (**b**) mitochondrial morphology in A549/Taxol cells; (**c**) enlarged detail of mitochondrion in A549 cell; (**d**) enlarged detail of mitochondrion in A549/Taxol cell; (**D**) quantitative polymerase chain reaction (PCR) analysis of relative transcript level of proteins regulating mitochondrial dynamics in A549 cells compared with A549/Taxol cells (n=3). The symbol * indicates the significant difference, *P*<0.05; ** indicates the significant difference, *P*<0.01.

The dominant functions of mitochondria are cellular respiration and energy generation. Mitochondrial damage leads to decreased oxidative phosphate activity and reduced ATP production. We first investigated intracellular ATP levels under regular high glucose circumstances, showing the ATP level in A549/Taxol cells was significantly lower than that in A549 cells. When incubated in a glycolysis inhibition environment for 24 hours, ATP levels in both cell lines witnessed a drastic drop.
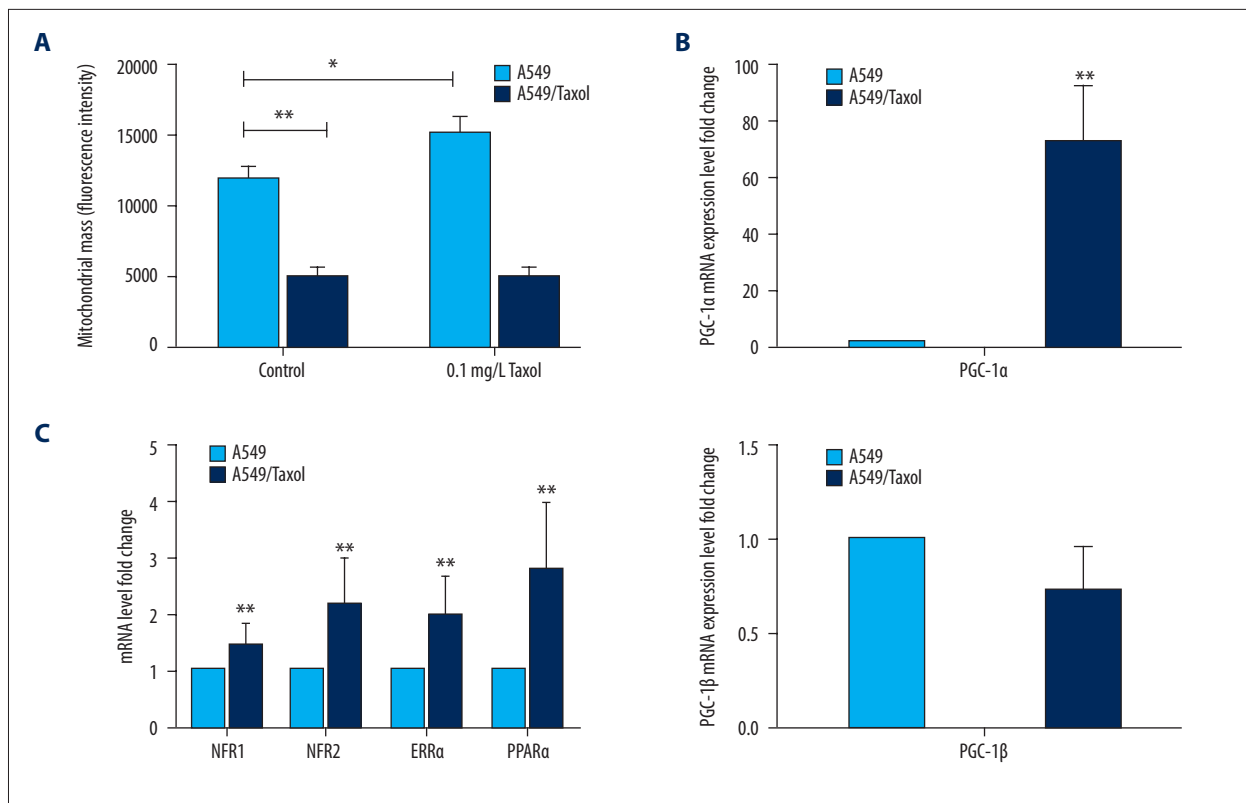
Figure 2. Characterization of mitochondrial mass and mitochondrial biogenesis alterations in paclitaxel-resistant cells. (**A**) Comparison of mitochondrial mass per cell under normal culture condition and paclitaxel treated condition (0.1 mg/L) in A549 and A549/Taxol cells. (**B**) Quantitative polymerase chain reaction (PCR) analysis of relative transcript level of PGC-1α (**upper**) and PGC-1β (**below**) in A549 and A549/Taxol cells (n=3). (**C**) Quantitative PCR analysis of relative transcript level of PGC-1α target proteins in A549 and A549/Taxol cells (n=3).

ATP production in A549 cells was reduced by almost 85%, while this was closer to 50% in A549/Taxol cells (Figure 3C). To further confirm this observation, the glucose utilization and lactate production were measured, showing that both processes decreased in A549/Taxol cells (Figure 3D). These results indicated that the A549/Taxol cells were less dependent on glycolysis for energy utilization compared to A549 cells.

We further investigated mitochondrial respiration with Seahorse XF24 Analyzer. OCR and ECAR indexes could reflect the rate of mitochondrial OXPHOS activity and the rate of lactic acid production via glycolysis, respectively. The basal respiration states were measured before addition of any modulators. The OCR baselines were 129.58±12.14 pMoles/min/10^5 cells for A549 and 90.40±11.20 pMoles/min/10^5 cells for A549/Taxol, and the ECAR baselines were 18.61±2.30 mpH/min/10^5 cells for A549 and 7.64±3.92 mpH/min/10^5 cells for A549/Taxol (Figure 3E). We measured the OCR index immediately after oligomycin, FCCP and rotenone/antimycin were sequentially added, and determined the reserve respiratory capability and the cellular RCR [26]. The cellular RCR is calculated as the value of respiratory state 3 dividing by that of respiratory state 4. The OCR

measured after FCCP injection could be considered equivalent to respiration state 3, while OCR measured after oligomycin injection as respiratory state 4. A549 cells showed significantly elevated OCR values during basal and inhibitor-treated respiration (Figure 3F). Interestingly, the reserve respiratory ability did not show any significant decrease in A549/Taxol cells. Meanwhile, the RCR of A549/Taxol cells was even higher than that of A549 cells, with values of 2.28±0.63 and 1.46±0.47, respectively (*P*<0.05). Although the basal respiratory profile was decreased, this may not imply that mitochondrial respiratory function was impaired in A549/Taxol cells since its mitochondrial mass was also significantly decreased. Higher reserve capability and RCR value indicated that mitochondrial function in A549/Taxol cells might be enhanced.

Discussion

Since Otto Warburg proposed the mitochondrial defective theory in cancer cells in last century, recent reports have demonstrated that mitochondrial function was not impaired in several cancer cell lines. Mitochondrial functions that contribute
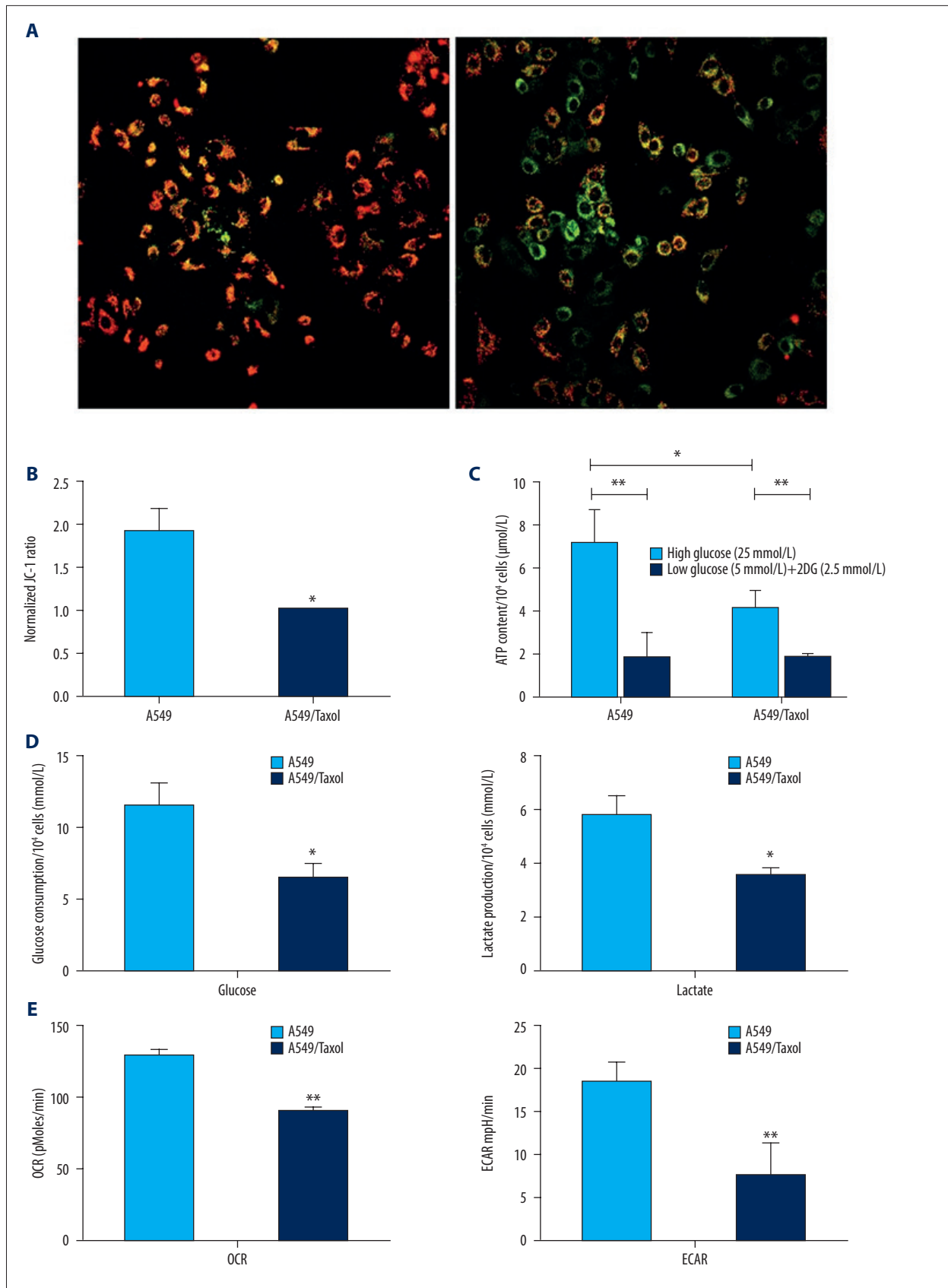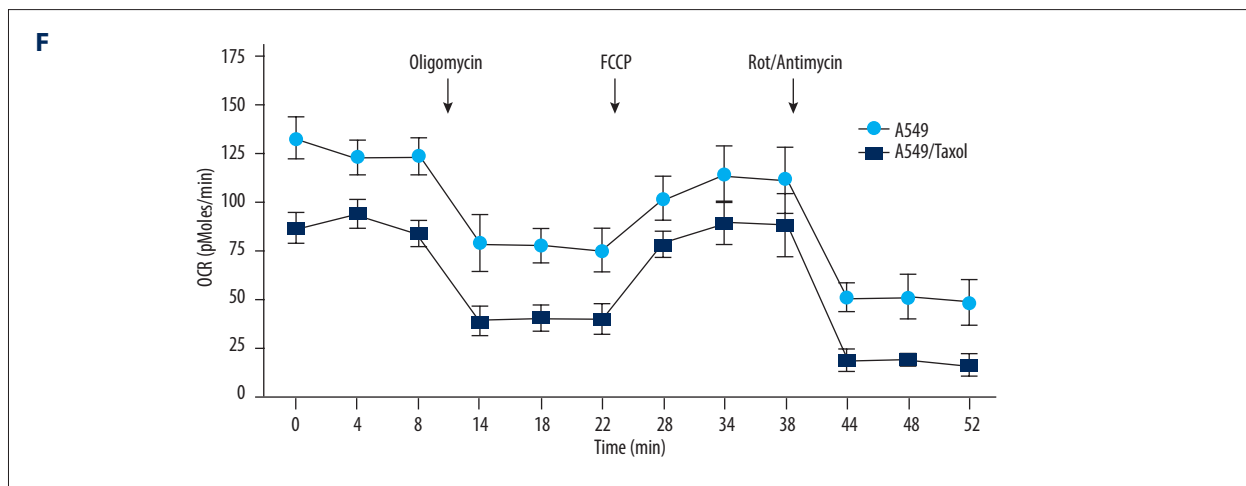
Figure 3. Characterization of cellular metabolic and mitochondrial functional alterations in paclitaxel-resistant cells. (**A**) Representative confocal microscopic images of $\Delta\psi_m$ labeled with JC-1 in A549 and A549/Taxol cells. (**B**) Flow cytometric measurement of $\Delta\psi_m$ with JC-1 in A549 and A549/Taxol cells. The JC-1 ratio is calculated as the ratio of red fluorescence intensity to green fluorescence intensity (n=3). (**C**) Comparison of ATP production level in 48 hours under normal culture condition (high glucose, 25 mmol/L) and glycolysis inhibition condition (low glucose, 5 mmol/L and 2DG (2-deoxy-D-glucose) treatment, 2.5 mmol/L) between A549 and A549/Taxol cells (n=3). (**D**) Determination of glucose consumption level (**left**) and lactate production level (**right**) in 24 hours in A549 and A549/Taxol cells (n=3). (**E**) Comparison of basal oxygen consuming rate (OCR) (**left**) and extracellular acidification rate (ECAR) (**right**) between A549 and A549/Taxol cells using Seahorse XF24 (n=3). (**F**) Respiratory profiles of cells in response to sequential administration of modulators (n=3).

to cancer are diverse but interconnected, including interfering with energy metabolism, reactive oxygen species generation, and induction of cellular stress responses. In cancer cells of the liver, ovarian and brain, mitochondrial malfunctions have been observed to be associated with resistance to certain alkylating drugs [27,28].

Our work reveals a series of changes of mitochondrial characteristics in A549/Taxol cells. Mitochondrial structures could readily adapt to different intracellular and extracellular conditions [29]. First, by visual observation of mitochondrial morphology and measurement of mitochondrial dynamic genes, we demonstrated that the mitochondrial dynamic balance shifted towards fusion in A549/Taxol cells. Mitochondrial fission takes part in the programmed cell death, and associates with the fragmented morphology of injured mitochondria that can be targeted for degradation [30]. On the contrary, mitochondrial fusion increases ATP generation efficiency and helps mitochondria to escape autophagy [31]. Tondera et al. suggested mitochondria would fuse into a closer network when cells are under modest stress. This elongated mitochondrial network confers certain resistance to harmful stimulations [32]. Our findings showed that mitochondria in A549/Taxol adopted a more fused morphology through the formation of elongated and interconnected mitochondrial tubules.

Mitochondrial fusion and fission are also important for the normal function of mitochondria. Mitochondrial fusion activity is mainly regulated by Mfn1, Mfn2, and OPA1 proteins. Mfn1 and

Mfn2 proteins mediate the fusion of outer membranes; OPA1 is involved in the regulation of mitochondrial inner membrane. Fis1 and Drp1 are the major proteins regulating mitochondrial fission. These proteins can mediate multiple signaling pathways to achieve resistance to apoptosis [14]. This observation was further confirmed by quantitative determination of dynamic genes. Elevated expressions of Mfn1 and Mfn2 in our data were strongly associated with mitochondria fusion in A549/Taxol cells. High expression of Mfn1 and Mfn2 promotes mitochondrial morphological changes and leads to apoptosis resistance, resistance to paclitaxel. Fis1 and Drp1 are the major proteins regulating mitochondrial fission. High expression of Fis1 and Drp1 promotes mitochondrial fission leading to apoptosis. In contrast, the low expression of Fis1 and Drp1 helps to inhibit cell apoptosis. [33]. Fis1 mRNA transcript level was downregulated in the A549/Taxol cell line, indicating the fission process was inhibited. Decreased expression of Fis1 inhibits mitosis in A549/T cells, which contributes to apoptosis resistance. Thus, a likely explanation for the increase of mitochondrial size and morphological elongation was that A549/Taxol cells adjusted its mitochondrial network into a more fused state and fission inhibition, which might help cancer cells against harmful stresses caused by chemotherapy.

The current study demonstrated that mitochondrial mass was significantly lower in A549/Taxol cells than in A549 cells. It was reported that paclitaxel pretreatment would result in a significant increase in mitochondrial mass in mammalian cells [34]. After short-term paclitaxel treatment, mitochondrial mass in

A549 cells witnessed an obvious increase, which was consistent with former report. But our data indicated that mitochondrial mass in A549/Taxol cells undergo an opposite response during long-term treatment with paclitaxel. Mitochondrial mass was significantly lower in A549/Taxol cells than in A549 cells. However, the reason that mitochondrial mass in A549/Taxol cells drastically decreased is unclear.

Although the mitochondrial mass is reduced, our research shows the transcription level of PGC-1α increased significantly in A549/Taxol cells. PGC-1α acts as a co-regulatory factor and is commonly found in large multiprotein complexes to attract transcription factors (NRF1, NRF2α, YY1, and MEF2C acting directly in the electron transport chain) and nuclear receptors (ERRα, ERRα, PPARα, and FXR) promotes mitochondrial biogenesis. PGC-1α is activated by stimulation of nutrient deprivation, oxidative damage and chemotherapy. PGC-1α antagonizes cell death by interacting with specific nuclear transcription factors (NRF1, NRF2, and ERRα) to affect mitochondrial respiration, reactive oxygen species defense system, and fatty acid metabolism [35,36]. Activation of PGC-1α promotes biosynthesis of tumor cells and induces resistance to chemotherapeutic drugs. Our study revealed the expression of PGC-1α and downstream genes increased in cancer cells in response to chronic paclitaxel toxicity. In this case, mitochondrial biogenesis pathway was stimulated to compromise and maintain the healthy mitochondria in paclitaxel-resistant cancer cells.

Mitochondrial plasticity, including fusion/fission events, biogenesis and clearance, could largely affect cellular energy homeostasis. A concomitant decrease in glucose consumption, lactate production, and ATP content were observed in A549/Taxol cells. Metabolic profiles of cells were further exemplified by mitochondrial stress test. The glycolysis and OXPHOS activity levels were both lower in A549/Taxol cells than that in A549 cells; and this metabolic reprogramming was also proven in our previous work using a flux assay [10,37]. However, the reaction of mitochondria to respiratory modulators indicated mitochondrial respiratory function was not impaired in A549/Taxol cells. The decreased basal respiratory levels might result from its lower mitochondrial mass. Our results indicated that paclitaxel acts on cancer cell metabolism through a totally different mechanism. Interestingly, cancer cells resistant to DNA alkylator drugs were hypersensitive to microtubule disassembly drugs. This little understood phenomenon also supports the idea that chemotherapeutic agents with varying pharmacological action may lead to chemo-resistance phonotypes through different mechanisms.

The present study provides a profile of mitochondrial alterations in paclitaxel-resistant lung cancer cells. The decreased proliferation capacity and lower metabolic level of A549/Taxol cells resembles the characteristics of senescence cells. It is noteworthy that mitochondrial elongation has been associated with cell senescence elongation, which shows increased mitofusion and reduced DRP1 and Fis1 expression [38–41]. Since a senescence-like phenotype after drug treatment has been identified as an important determinant in the outcome of cancer chemotherapy, it might be possible that mitochondria play a certain role in chemoresistance through cellular senescence [42,43]. However, further studies are essential to clarify the underlying relationship. Our work suggests that abnormal mitochondria might be an adaptive transition in cancer cells to harmful stresses caused by chemotherapy. Research on mitochondrial transformation could provide new insights into the essence of drug resistance and allow for the development of innovative therapeutic strategies.

Conclusions

Our study reveals a series change of mitochondrial characteristics in paclitaxel-resistant cells. Mfn1 and Mfn2 and PGC-1α increased, while Fis1 expression and mitochondrial oxidative phosphorylation decreased in A549/Taxol cell lines. These changes of mitochondrial fusion, fission, and biological function contributes to the occurrence of paclitaxel resistance in tumor cells which induce paclitaxel resistance. These results will help aid our understanding of paclitaxel resistance and will be useful for predicting occurrence of paclitaxel resistance and reversing drug resistance by targeting Mfn, Fis1, and PGC-1α genes and mitochondrial oxidative phosphorylation.

Conflict of interest

None.

This work is licensed under Creative Common Attribution-
NonCommercial-NoDerivatives 4.0 International (CC BY-NC-ND 4.0)

e918216-9

Indexed in: [Current Contents/Clinical Medicine]   [SCI Expanded]   [ISI Alerting System]
[ISI Journals Master List]   [Index Medicus/MEDLINE]   [EMBASE/Excerpta Medica]
[Chemical Abstracts/CAS]

References:

1. Siegel RL, Miller KD, Jemal A: Cancer statistics, 2019. A Cancer J Clin, 2019; 69(1): 7–34

2. Travis WD, Brambilla E, Burke AP et al: Introduction to the 2015 World Health Organization classification of tumors of the lung, pleura, thymus, and heart. J Thorac Oncol, 2015; 10(9): 1240–42

3. Li P, Liu H, Zhang Z et al: Expression and comparison of Cbl-b in lung squamous cell carcinoma and adenocarcinoma. Med Sci Monit, 2018; 24: 623–35

4. Punzi S, Meliksetian M, Riva L et al: Development of personalized therapeutic strategies by targeting actionable vulnerabilities in metastatic and chemotherapy-resistant breast cancer PDXs. Cells, 2019; 8(6): pii: E605

5. Ledermann JA: Front-line therapy of advanced ovarian cancer: New approaches. Ann Oncol, 2017; 28(Suppl.): viii46–50

6. Zhang Y, Yang B, Zhao J et al: Proteasome inhibitor carbobenzoxy-L-leucyl-L-leucyl-L-leucinal (MG132) enhances therapeutic effect of paclitaxel on breast cancer by inhibiting nuclear factor (NF)-kappaB signaling. Med Sci Monit, 2018; 24: 294–304

7. Kavallaris M: Microtubules and resistance to tubulin-binding agents. Nat Rev Cancer, 2010; 10: 194–204

8. Peng M, Darko KO, Tao T et al: Combination of metformin with chemotherapeutic drugs via different molecular mechanisms. Cancer Treat Rev, 2017; 54: 24–33

9. Nunnari J, Suomalainen A: Mitochondria: In sickness and in health. Cell, 2012; 148(6): 1145–59

10. Zhou X, Chen R, Yu Z et al: Dichloroacetate restores drug sensitivity in paclitaxel-resistant cells by inducing citric acid accumulation. Mol Cancer, 2015; 14: 63

11. Wallace DC: Mitochondria and cancer. Nat Rev Cancer, 2012; 12(10): 685–98

12. Pasquier J, Guerrouahen BS, Al Thawadi H et al: Preferential transfer of mitochondria from endothelial to cancer cells through tunneling nanotubes modulates chemoresistance. J Transl Med, 2013; 11: 94

13. Chan CY, Pedley AM, Kim D et al: Microtubule-directed transport of purine metabolons drives their cytosolic transit to mitochondria. Proc Natl Acad Sci USA, 2018; 115(51): 13009–14

14. Lee H, Yoon Y: Mitochondrial fission and fusion. Biochem Soc Trans, 2016; 44(6): 1725–35

15. Sun QL, Sha HF, Yang XH et al: Comparative proteomic analysis of paclitaxel sensitive A549 lung adenocarcinoma cell line and its resistant counterpart A549-Taxol. J Cancer Res Clin Oncol, 2011; 137(3): 521–32

16. Brand MD, Nicholls DG: Assessing mitochondrial dysfunction in cells. Biochem J, 2011; 435(2): 297–312

17. Yang CH, Horwitz SB: Taxol(R): The first microtubule stabilizing agent. Int J Mol Sci, 2017; 18(8): pii: E1733

18. Vitale SG, Lagana AS, Nigro A et al: Peroxisome proliferator-activated receptor modulation during metabolic diseases and cancers: Master and minions. PPAR Res, 2016; 2016: 6517313

19. Scarpulla RC: Metabolic control of mitochondrial biogenesis through the PGC-1 family regulatory network. Biochim Biophys Acta, 2011; 1813(7): 1269–78

20. Jones AW, Yao Z, Vicencio JM et al: PGC-1 family coactivators and cell fate: Roles in cancer, neurodegeneration, cardiovascular disease and retrograde mitochondria-nucleus signalling. Mitochondrion, 2012; 12(1): 86–99

21. Correia RL, Oba-Shinjo SM, Uno M et al: Mitochondrial DNA depletion and its correlation with TFAM, TFB1M, TFB2M and POLG in human diffusely infiltrating astrocytomas. Mitochondrion, 2011; 11(1): 48–53

22. Hou Z, O'Connor C, Fruhauf J et al: Regulation of differential proton-coupled folate transporter gene expression in human tumors: Transactivation by KLF15 with NRF-1 and the role of Sp1. Biochem J, 2019; 476(8): 1247–66

23. Basak P, Sadhukhan P, Sarkar P, Sil PC: Perspectives of the Nrf-2 signaling pathway in cancer progression and therapy. Toxicol Rep, 2017; 4: 306–18

24. Madhu Krishna B, Chaudhary S, Mishra DR et al: Estrogen receptor alpha dependent regulation of estrogen related receptor beta and its role in cell cycle in breast cancer. BMC Cancer, 2018; 18(1): 607

25. Battogtokh G, Choi YS, Kang DS et al: Mitochondria-targeting drug conjugates for cytotoxic, anti-oxidizing and sensing purposes: Current strategies and future perspectives. Acta Pharm Sin B, 2018; 8(6): 862–80

26. Modis K, Gero D, Erdelyi K et al: Cellular bioenergetics is regulated by PARP1 under resting conditions and during oxidative stress. Biochem Pharmacol, 2012; 83(5): 633–43

27. Bosc C, Selak MA, Sarry JE: Resistance is futile: targeting mitochondrial energetics and metabolism to overcome drug resistance in cancer treatment. Cell Metabol, 2017; 26(5): 705–7

28. Peng YB, Zhao ZL, Liu T et al: A multi-mitochondrial anticancer agent that selectively kills cancer cells and overcomes drug resistance. ChemMedChem, 2017; 12(3): 250–56

29. Westermann B: Bioenergetic role of mitochondrial fusion and fission. Biochim Biophys Acta, 2012; 1817(10): 1833–38

30. Guo MY, Shang L, Hu YY et al: The role of Cdk5-mediated Drp1 phosphorylation in Abeta1-42 induced mitochondrial fission and neuronal apoptosis. J Cell Biochem, 2018; 119(6): 4815–25

31. Huang Q, Zhan L, Cao H et al: Increased mitochondrial fission promotes autophagy and hepatocellular carcinoma cell survival through the ROS-modulated coordinated regulation of the NFKB and TP53 pathways. Autophagy, 2016; 12(6): 999–1014

32. Tondera D, Grandemange S, Jourdain A et al: SLP-2 is required for stress-induced mitochondrial hyperfusion. EMBO J, 2009; 28(11): 1589–600

33. Shen Q, Yamano K, Head BP et al: Mutations in Fis1 disrupt orderly disposal of defective mitochondria. Mol Biol Cell, 2014; 25(1): 145–59

34. Farnie G, Sotgia F, Lisanti MP: High mitochondrial mass identifies a subpopulation of stem-like cancer cells that are chemo-resistant. Oncotarget, 2015; 6(31): 30472–86

35. Di W, Lv J, Jiang S et al: PGC-1: The energetic regulator in cardiac metabolism. Curr Issues Mol Biol, 2018; 28: 29–46

36. Deblois G, St-Pierre J, Giguere V: The PGC-1/ERR signaling axis in cancer. Oncogene, 2013; 32(30): 3483–90

37. Li J, Zhao S, Zhou X et al: Inhibition of lipolysis by mercaptoacetate and etomoxir specifically sensitize drug-resistant lung adenocarcinoma cell to paclitaxel. PLoS One, 2013; 8(9): e74623

38. Gomes LC, Di Benedetto G, Scorrano L: During autophagy mitochondria elongate, are spared from degradation and sustain cell viability. Nat Cell Biol, 2011; 13(5): 589–98

39. Hasnat M, Yuan Z, Naveed M et al: Drp1-associated mitochondrial dysfunction and mitochondrial autophagy: A novel mechanism in triptolide-induced hepatotoxicity. Cell Biol Toxicol, 2019; 35(3): 267–80

40. Mai S, Klinkenberg M, Auburger G et al: Decreased expression of Drp1 and Fis1 mediates mitochondrial elongation in senescent cells and enhances resistance to oxidative stress through PINK1. J Cell Sci, 2010; 123(Pt 6): 917–26

41. Yu R, Jin SB, Lendahl U et al: Human Fis1 regulates mitochondrial dynamics through inhibition of the fusion machinery. EMBO J, 2019; 38(8): pii: e99748

42. Achuthan S, Santhoshkumar TR, Prabhakar J et al: Drug-induced senescence generates chemoresistant stemlike cells with low reactive oxygen species. J Biol Chem, 2011; 286(43): 37813–29

43. Guerra F, Arbini AA, Moro L: Mitochondria and cancer chemoresistance. Biochim Biophys Acta Bioenerg, 2017; 1858(8): 686–99